Islanding Detection and Enhancement of Microgrid Performance

Aref Pouryekta , *Student Member, IEEE*, Vigna K. Ramachandaramurthy, *Senior Member, IEEE*,
Nadarajah Mithulananthan , *Senior Member, IEEE*, and Atputharajah Arulampalam, *Senior Member, IEEE*

Abstract—Nowadays, renewable energy sources (RES) are widely used in the distribution system. Despite the advantages of RES in the system, they also introduce some problems such as unintentional islanding, protection concerns, reverse power flow, etc. Due to the unpredictable faults or scheduled maintenance plans, a distribution system can be sectionalized into several islands provided that enough dispersed generation units are available. Thus, distribution systems should be capable of detecting islanding condition for smooth transition to an islanded mode. As a first step, an islanding detection method (IDM) is proposed in this paper to detect the islanding phenomenon in a distribution system. The proposed method is a hybrid IDM which consists of a remote detection method and a passive method. In the next step, an adaptive control strategy is proposed to ensure stable operation of islanded subsections. The proposed method utilizes error rates of system parameter such as voltage and power to readjust generator controllers and maintain the system stability. The proposed IDM and adaptive controller are implemented on a generic distribution network using EMTDC/PSCAD software. Results have shown that the hybrid detection method is capable of detecting the islanding in the presence multiple distributed generation units. Moreover, the proposed IDM is not affected by load/generation changes. Results also showed a smooth transition from grid-connected mode to autonomous operation mode. Furthermore, the proposed adaptive control strategy maintains stable operation of the island when fault occurs in the island.

Index Terms—Control of islands, islanding detection, power control, renewable energy resources, voltage control.

I. INTRODUCTION

IN RECENT decades, global warming and environmental concerns alongside privatization and deregulated electricity market have encouraged utilities to utilize renewable energy sources (RESs). In conventional distribution systems, which are radially configured, power flows in one direction from the main substation into the downstream loads. However, in the modern distribution systems with RESs, bidirectional power flow occurs. This situation has substantial impact on the protection system as load can be supplied from multiple sources and direction. Moreover utilizing RES in distribution network affects the system parameters such as voltage and frequency since RESs are intermittent in nature. Furthermore, most of the RES-based dispersed generator (DG) units need a power electronic interface to convert the renewable energy into electrical energy, which introduces harmonics. Due to the high penetration of RES in distribution systems, islanded operation mode of DG units is considered by many utilities as a suitable approach to maintain continuity and reliability. However, islanded operation requires fast, precise, and cost-effective islanding detection method (IDM), which does not affect the quality of supply. Hence, various types of IDMs and different control strategies have been developed and deployed on these DG units. In accordance to IEEE Std 1547-2003 [1], islanding should be detected within 2 s after it occurs. IDMs can be classified into three types, namely passive detection method (PDM), active detection method (ADM), and remote detection method (RDM).

The PDMs are based on measuring parameters such as voltage and frequency at the point of common coupling (PCC). Several passive methods such as over/under voltage/ frequency [2]–[10], rate of change of frequency (ROCOF) [11], [12], ROCOF over power [12], harmonic monitoring [6], [12], phase jump detection [6], [12], [13], and voltage vector shift [12], [14], [15] have been developed to detect the islanding phenomenon. In PDMs, observing any violation from normal values is considered as islanding. The advantages of these methods include simplicity and low cost of implementation as they use conventional metering and protection devices to detect islanding. Moreover, PDMs do not affect the power quality and conforms to the 2 s detection time. However, the main drawback is that the PDMs have large nondetection zone (NDZ), which leads to failure in islanding detection when load and power generation are balanced. Another drawback is the possibility of wrong detection during large load/generation variation or faults, whereas these contingencies can cause PCC parameters violet the thresholds [16].

The performance of ADM is based on perturbation and observation concept. A DG parameter is chosen to be distorted by injecting perturbation. In the presence of a stiff grid, the amplitude of the variation at the PCC is negligible since the grid parameters are dominant. However, injecting disturbance into the PCC results in significant variation on DG parameters during the islanding phenomenon. Several active methods such as impedance measurement [11], [17]–[20], active frequency drift [2], [11], [21]–[23], frequency jump [11], Sandia frequency shift [6], [11], [12], [24]–[27], sliding mode frequency shift [2], [11],

[12], [24], [28], [29], phase distortion method [12], [30], [31], harmonic injection method [11], [29], [32], [33], Sandia voltage shift [12], [24], [34], power variation monitoring [11], [12], and reactive power export error detection [12], [20], [35]–[37] are developed to detect the islanding. The NDZ area for ADMs is remarkably reduced to a very small value or even zero compared to the PDMs. However, there are several drawbacks for ADMs such as:

1) reduction in power quality via injecting distortion into the system;
2) possibility of interfering of distortion signals in the presence of multiple DG units;
3) possibility of misdetection when there is a combination of synchronous generators and power electronic interface-based sources;
4) most of the ADMs are developed for inverter-based DG units and are not applicable for synchronous generators.

The remote-based detection method theoretically has no NDZ and introduces just one disturbance source into the system compared to ADMs. Several RDM such as supervisory control and data acquisition [11], [21], [35], [38], power line carrier signaling [11], [39]–[41] and signal produced by disconnect [11], [29], [42] are developed to detect the islanding. The RDM are developed to overcome the problems faced by passive and active methods. The RDMs employ a communication pattern between DG unit and main grid to alert and disconnect the DG units once unintentional islanding takes place. These methods do not have NDZ. Furthermore, RDMs are applicable to the systems with multiple DG units which include both inverter-based sources and synchronous generators. The main drawback for RDMs is the cost since these methods require a communication platform to send islanding detection signals (IDSs).

In general, hybrid detection methods (HDM) combine the features of aforementioned techniques to increase the detection accuracy [43], [44]. The HDMs are developed in order to overcome drawbacks of local and RDMs and improve their performance. For example, signal processing techniques are utilized by the other IDMs in order to analyze the characteristics of the measured parameters [12], [45], [46]. The signal processing techniques effectively extract the unseen information from the measured signals to detect the islanding. Extracting this hidden information reveals the parameters that violate the threshold. Moreover, the NDZ is reduced using these techniques. Combining the local IDMs with RDMs results in the more accurate detection.

As a first step in this paper, an HDM, which is a combination of RDM and PDM, is proposed to overcome the mentioned drawbacks. The utilization of the rate of change of voltage phase (ROCOVP) as a passive method increases the accuracy of the signal detector (SD) to ensure the receiver is able to extract the weak signals.

Once Islanding occurs, the ability of the DG units to sustain the transition is a key point to maintain the stability of the islanded section [47], [48]. Several control method are proposed by different authors [49]. The existing control architectures uses fix PI controls in their control structure. The fix PI controllers do not reflect the system changes and they are not adoptable with
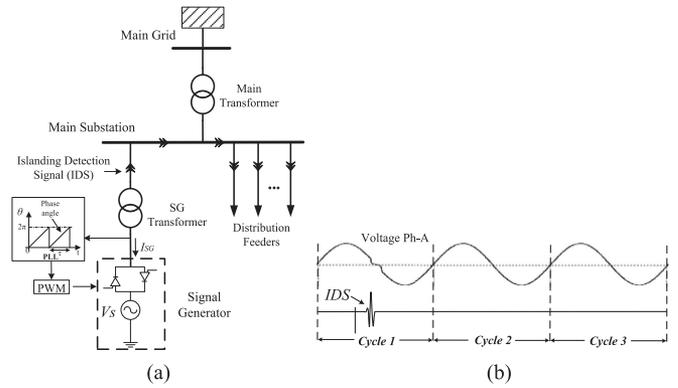
Fig. 1.   (a) Single-line diagram of the SG connected between phase A and ground and (b) IDS in every three cycles.

new system configuration. In order to overcome this problem, a new adaptive control is proposed in this paper.

Once islanding is detected, an adaptive PI controller-based strategy is proposed to ensure continuous power supply in the island. Adaptive PI controller utilizes voltage, frequency, and power error rates to improve the control system performance during the grid-connected and autonomous operation modes. In the proposed method, PI controller gains change dynamically according to the rate of generator output errors to stabilize the DG units during various contingencies.

This paper is organized as follows: Section II presents the proposed HDM. Section III elaborates the droop control structure of the generators and adaptive PI controller. In Section IV, a practical test network is addressed to validate the proposed method. Simulation results are investigated in Section V while the conclusion is presented in Section VI.

II. Proposed Islanding Detection

In order to overcome the aforementioned drawbacks of the detection methods, the power line signaling method proposed in [39] is combined with a novel PDM. Due to the damping feature of the power network, IDSs may not be visible at the PCC. Two possible solutions to solve this problem:

1) increasing the strength of the IDSs by adopting a higher rated signal generator (SG) (not recommended);
2) using more efficient signal detection method (recommended).

Hence, the ROCOVP is proposed as a more efficient detection method to extract the IDSs. Hence, the proposed HDM is capable of detecting weak signals during different contingency situations in the system.

A. SG

SG is used to generate the IDSs every three cycles. IDS's can be sent between one phase and ground or between two phases. Fig. 1(a) demonstrates the SG placed in the main substation between phase A and ground [39]. System parameters such as grid impedance, DG impedance and reactive power compensators affect the IDSs. In order to reduce the influence of the system parameters, IDS strength can be increased using
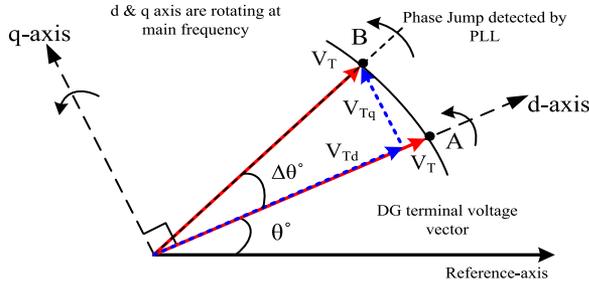
Fig. 2.   Phasor diagram of phase jump detection on the DG busbar.

Fig. 3.   PLL model for angle detection.

different triggering angles for the thyristors. Strong IDS makes it easy to detect in distribution networks; however, it introduces harmonics and requires a higher rated SG transformer. Sending IDS in short intervals reduces the injected harmonics. Moreover, utilizing efficient detection algorithms results in detecting even weak IDS. Hence, lower rating transformer can be used for the SG. Fig. 1(b) shows the phase A voltage carrying IDS every three cycles. In order to decrease the SG current, pulse width modulation pulses trigger the thyristors near the zero crossing of voltage waveform. The peak value of the IDS at the main substation can be determined using

$$V_{\text{Signal-peak}} = \sqrt{\frac{2}{3}}\, U_L \frac{L_{\text{self}}}{L_{\text{self}} + L_T} \sin(\delta). \qquad (1)$$

V_L is the line-to-line voltage, L_{self} is the main grid impedance, L_T is the SG transformer impedance, and δ is the trigger angle of the thyristors. In order to define the strength of the IDS, k, ratio of its peak value to the peak of its carrier is used [39]

$$k = \frac{V_{\text{signal-peak}}}{V_{\text{PG-peak}}} = \frac{L_{\text{self}}\sin\delta}{L_{\text{sefl}} + L_T} = \frac{X_{\text{self}}\sin\delta}{X_{\text{self}} + X_T} \cdot 100\%. \quad (2)$$

The $V_{\text{PG-peak}}$ is the peak value of the carrier voltage waveform. Moreover, the maximum total levels of harmonic distortion (THD) at any connection point on the distribution system from all sources shall not exceed 6.5% at 11 kV [50].

B. SD

There are several methods to detect the IDS, such as comparing the received signal with a reference signal and monitoring the harmonics [39]. Since previous methods are affected by the events such as generators "Start Event" and "Large Load Change Event," this paper proposes to monitor the ROCOVP to detect the islanding. Using Parks transform, the d–q frame voltage can be calculated. Fig. 2 demonstrates the phase jump in d–q frame. When the IDS reach the DG unit busbar, V_T jumps from points A to B and the voltage angle shifts to a new value. Therefore, a change in V_{Tq} reveals the presence of IDS. Using a phase-locked loop (PLL), phase jumps can be detected and IDS can be extracted. Schematic diagram of the PLL configuration is shown in Fig. 3.

As mentioned in the previous section, voltage fluctuation due to large load variation or generation variation affect the V_{signal} and it may result in wrong islanding detection and trip DG units
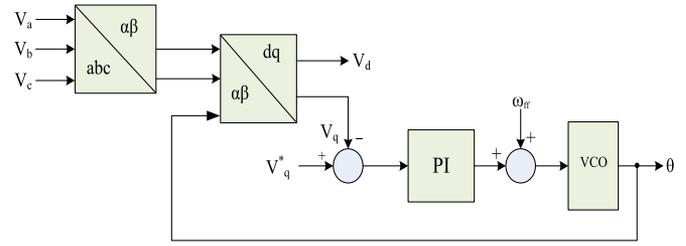
without real islanding phenomenon. In order to extract the IDSs during the voltage fluctuations, phase factor (*PhF*) is proposed. *PhF* is defined using

$$PhF = \frac{\Delta\theta}{\Delta t} = \frac{\theta_2 - \theta_1}{t_2 - t_1}. \qquad (3)$$

Since the V_{Tq} is directly related to the phase of the voltage, *PhF* can be calculated as follows:

$$\Delta\theta = \sin^{-1}(V_{Tq}/V_T) \Rightarrow$$

$$PhF = \frac{\sin^{-1}(V_{Tq}/V_T)}{\Delta t}. \qquad (4)$$

The proposed phase factor results in more accurate IDS extraction as shown in the results section. The PhF has the ability to detect low strength IDS at PCC. The ability of detecting the low strength signals improves the power quality since the negative influence of the SG on the system is reduced by decreasing the trigger angle, δ. Moreover, the increase in signal detection accuracy will lower the equipment ratings and cost of the SG. Noises and different faults may corrupt the IDS and lead to wrong islanding detection. According to the IEEE Std. C37.119 and IEEE Std. 1547, the protection system should remove the fault within (five to eight cycles). Regardless of the fault type, the circuit breakers disconnect the faulty line section within the specific time. In order to ensure that the proposed detection method is not affected by the fault, an island is formed when four consecutive IDSs are not detected. For every three cycles, one IDS is received. Hence, losing four consecutive IDS represents 12 cycles. Hence, during this time, the faulty section is already cleared by the protection system. The ability to detect low strength signals allows the SG to inject a weaker distortion signal. Hence, the power quality is improved. Moreover, an SG with lower rating can be employed, thus decreasing the cost. This method can also be utilized for islanding detection in distribution systems for both inverters-based and synchronous generator-based DG units.

The proposed HDM has shown a high performance in islanding detection. In contrary to the local detection methods, the proposed method overcomes the main drawbacks of passive and ADMs. The proposed HDM not only has no NDZ, but is able to detect islanding in the presence of multiple DG units. Moreover, the proposed method is applicable for islanding detection for both voltage-source convertors and synchronous generator-based DG units. Comparison of the proposed method with the method in [39] reveals its capability to detect weak

TABLE I
COMPARISON OF THE ISLANDING DETECTION USING THE
PROPOSED METHOD AND XU METHOD

	Proposed HDM method	Xu method (PLCS) [39], [51]
Detection time	200 ms	200 ms
Detectable signal strength ($k\%$)	0.83%	4%
Minimum trigger angle for SG thyristors	15°	25°
Power quality	Negligible	Very small impact
Cost	Lesser than PLCS	High

Fig. 5. Schematic diagram of the control system.

Fig. 6. Load sharing between two parallel generators.

and voltage of the island should be controlled. If the remaining loads exceed 110% of generation capacity, a load shedding strategy should be performed to balance the load and generation in separated subsections.

Fixed PI controller and adaptive PI controller are implemented and results are then compared. Implementing an adaptive control strategy ensures smooth transition to the autonomous operation mode. These methods will be explained in the next sections.

During autonomous operation mode, a new slack busbar is required inside the island. Depending on the type and the number of remaining DG units, at least one of the DG units operates as a master unit and the other DG units operate as slave unit. The master DG units are responsible for controlling the voltage and frequency and maintain the stability of the island. Fig. 5 represents the schematic diagram of the control system for master DG units. As demonstrated in Fig. 5, when islanding is formed, the control mode of the master DG units shifts from *P-Q* control mode to *P-V* control mode.

Fig. 4. Stabilizing the microgrid by means of IDM and DG controllers.

signals. Comparison between the proposed method and Xu's method is presented in Table I.

III. ARCHITECTURE OF THE CONTROL STRATEGIES

Once islanding takes place, at least one DG has to work in *P-V* mode to provide a reference point in the network. Fig. 4 shows the flowchart of islanding detection and the stabilization of the DG units. Once islanding takes place, for example, frequency

A. Control Loop for Output Active Power

Once islanding occurs, all generators respond to the load demand variation based on their droop curve. The load sharing between two synchronous generators are illustrated in Fig. 6. Equation (5) presents the relation of generated power from each DG units respect to their *P-f* drop coefficient.

Use of droop control prevents frequency conflicts between two parallel generators since they use different droop to control
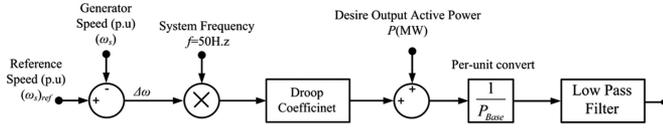
Fig. 7.   Active power control for DG units.
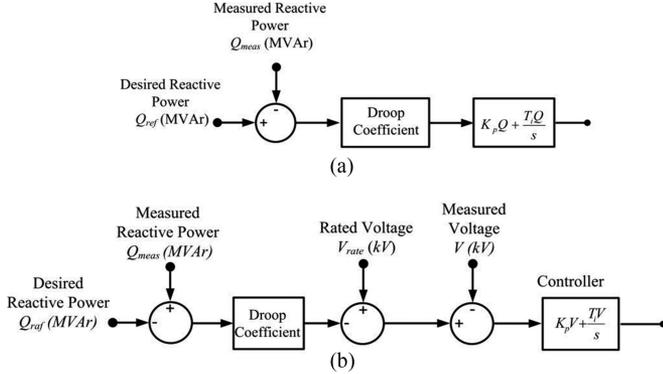
Fig. 8.   (a) Reactive power control loop and (b) voltage control loop for DG units.



Fig. 9.   Schematic diagram of (a) adaptive PI controllers to regulate the output reactive power and (b) adaptive control loop for voltage.

the output frequency

$$\frac{\Delta P_{G1}}{\Delta P_{G2}} = \frac{R_2}{R_1}. \tag{5}$$

The generators will maintain the frequency within $\pm 1\%$ of its rating value by means of $\pm 10\%$ change in output active power. Hence, output power can be controlled by utilizing the generator speed (ω_s, rad/sec) and input torque (τ). The power control loop is depicted in Fig. 7, where the output power of the master generator follows network load consumption. Equation (6a) and (6b) present the *P-f* droop coefficient for DG-1 and DG-2, respectively. Furthermore, due to disturbances such as faults and large load variation, the generator speed oscillates ($\omega_s \pm \Delta\omega$) around the operation point. Speed variation results in generator angle oscillation and causes angle stability issues. Thus, to prevent the angle oscillation, a low-pass filter is used in the speed control loop

$$R_{G1} = \frac{\Delta f\,(p.u)}{\Delta P_{G1}\,(p.u)} = \frac{f_0 - f'}{P'_{G1} - P_{0G1}} \tag{6a}$$

$$R_{G2} = \frac{\Delta f\,(p.u)}{\Delta P_{G2}\,(p.u)} = \frac{f_0 - f'}{P'_{G2} - P_{0G1}}. \tag{6b}$$

B. Control Loop of Voltage Output Reactive Power: In order to control the reactive power of the generators, droop control is used. Use of droop control allows the generator to work in different power factors (PFs). Hence, flexible PF permits the generator to follow the load PF based on its droop curve. Reactive power control loop is illustrated in Fig. 8(a).

After islanding, at least one source should be responsible for the voltage control. The voltage is controlled by the master DG unit via its voltage control loop. The PF can vary between 0.8 lagging to 0.9 leading in order to generate the reactive power

demand after islanding. The droop characteristic and feature of the reactive power control are shown in Fig. 8(b).

C. Adaptive PI Controller: Use of PI controller allows the safe transition into island mode. However, fluctuation of the generator parameters such as the speed and voltage is inevitable during disturbances. Decreasing the amplitude of the oscillations will result in higher stability margin during islanding operation. Therefore, calculating the $K_p V$, $T_i V$, $K_p Q$, and $T_i Q$ of the two adaptive PI controller becomes vital to obtain a stable output from PI controller and reach stable operation for the generator [52].

When the system topology changes due to islanding, the $K_p V$, $T_i V$, $K_p Q$, and $T_i Q$ determined previously may not necessarily be the optimal values. Hence, a new PI setting is required to decrease the over shoot and settling time of the system parameters such as frequency and voltage. New $K_p V$, $T_i V$, $K_p Q$, and $T_i Q$ will set the DG units output in such a way to decrease the rate of change of voltage or reactive power error signals. Fig. 9 demonstrates the adaptive PI control loops for reactive power and voltage regulation. When islanding takes place, rate of change of reactive power error and the rate of change of the voltage error signals will depend on the power demand in the island and the available generating capacity. When the imbalance between generated power and demand in the island is considerable, transient variation in the output parameters of the generator becomes significant. Adaptive PI controller consists of an adaptive PI controller and two auxiliary PI controllers. In the adaptive PI controller, the adaptive PI controller parameters are automatically adjusted using two auxiliary PI controllers.

Since for reactive power control, rate of change of reactive power error signal ($d(\Delta Q)/dt)$) is used to tune the $K_p Q$ and $T_i Q$ of the adaptive PI controller. Using ROCOVP for dynamic adjustment of the adaptive PI controller decreases the over/undershoot and oscillation in output reactive power and ensures the stable operation during the faults and disturbances.

Accordingly, for voltage control, rate of change of voltage error signal ($d(\Delta V)/dt)$) is used to tune the $K_p V$ and $T_i V$ of the adaptive PI controller. When the rate of change of error signal
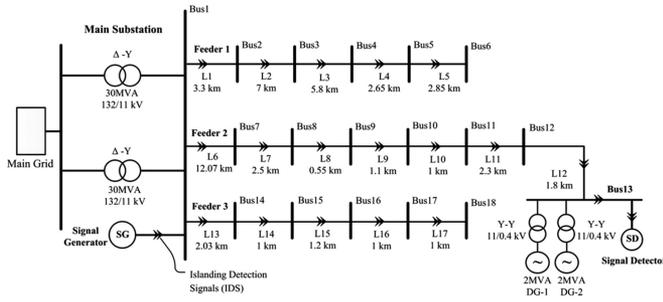
Fig. 10.   Practical 18 busbar distribution network.

Fig. 11.   Voltage of phase A at the PCC.

increases, the adaptive PI control gains are changed in order to make the error signal zero. In the proposed adaptive control technique, the adaptive PI controller gains are tuned automatically to obtain the optimum value and reduce the active power fluctuation as minimum as possible during and after islanding. As inertia of the islanded system is lesser than grid-connected mode, flexible settings for generators PI controllers ensure smooth transition from grid-connected mode to autonomous operation. Another advantage of using the proposed control is that adjustment of the auxiliary PI controllers is simpler and they can vary in wider range. Thus, with alternative PI gains, optimum functioning for Q and V control loops will be achieved.

IV. GENERIC TEST DISTRIBUTION SYSTEM

In order to investigate the proposed IDM and adaptive control technique for synchronous generator, a modified 11 kV, 50 Hz generic network from Malaysian electrical distribution utility is modeled using EMTDC/PSCAD. The single-line diagram of this network is presented in Fig. 10. The network has 18 busbars and 17 overhead lines. Both transformers in the main substation are 132/11 kV, Δ-Yg, rated at 30 MVA and impedance 10%. Fault level at 132 kV busbar is 14 and 17.8 kA at 11 kV. Two 2 MVA synchronous generators were used as DG units.

DG-1 as shown in Fig. 10 operates as a slave generator while DG-2 operates as a master generator. Master generator (DG-2) is equipped with droop voltage control to adjust the busbar voltage after islanding. Each generator is connected to the distribution network via 0.4/11 kV, 3 MVA, Yg-Yg and impedance 5% transformer. SG was connected to the network via single phase transformer 6.35/.22 kV, rated at 200 kVA and 3% impedance. Simulation results are discussed in detail in the next section.

V. RESULTS AND DISCUSSION

A case study of three events is investigated to verify the proposed IDM and control strategies. In this case study, three events are applied to the test distribution network. The first event is the "Start Event" of two DG units. Start Event is initiated by releasing the rotors of both synchronous machines at 1 s. Second event is "Large Load Change Event." Voltage disturbance occurs because of change in combination of dynamic motor loads and static loads at busbar 7 to 13 at 10 s. The third event is "Intentional Islanding Event." Intentional Islanding Event is initiated at feeder 2 via opening the line L6 in Fig. 10 at 20 s. The SG is installed at the main substation and
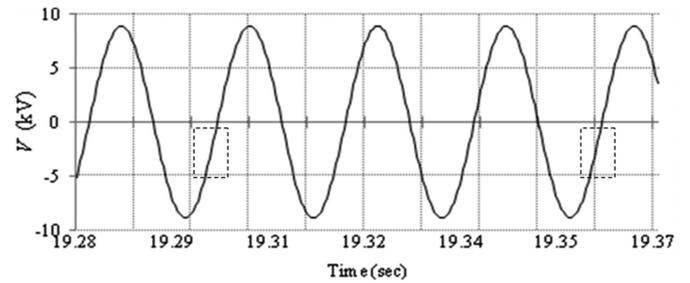
sends the IDS's to both downstream DG units with 0.06 s time interval. Thyristors are triggered at $\delta = 15°$ at the zero crossing point of the negative-going voltage.

A. Island detection

The phase A voltage is measured at PCC to extract the signals and to detect the islanding. As depicted in Fig. 11, IDS's have the least detrimental impact on the carrier voltage waveform at PCC.

Full window of the d-q frame voltage, which is modulated with IDSs at PCC, is illustrated in Fig. 12(a). Three different events are shown in Fig. 12(a) to investigate the proposed IDM. An expanded window of "Start Event" is shown in Fig. 12(b). Releasing both synchronous machines rotors imposes the voltage disturbance into the system.

As seen in Fig. 12(b), during the "Start Event," voltage fluctuation can lead to wrong detection. Next, "Large Load Change Event" causes voltage oscillation in the system.

Expanded window for "Large Load Change Event" is shown in Fig. 12(c), where it is seen that during voltage fluctuation, some IDS's are affected and cannot be extracted. Since losing four consecutive IDS's is considered as islanding, undetected IDSs during voltage disturbances lead to wrong islanding detection followed by the tripping of the DG units within the next 2 s. Hence, it is important to extract the IDS during the voltage disturbances. An expanded window for "Intentional Islanding Event" is shown in Fig. 12(d). As can be seen, the IDS's were not received after islanding as the connection between an SG and a SD is lost due to intentional islanding. Increasing the strength of the signal or utilizing more accurate extraction method can be taken into account to make the IDS detectable during the events. Increasing the strength of IDS imposes higher distortion to the system and requires bigger interface transformer for the SG. The ROCOVP method is proposed to detect IDS's during the events. A full window of extracted IDS's using the proposed ROCOVP method is depicted in Fig. 13(a). Phase factor is shown in Fig. 13(a) during three different events. Expanded window of "Start Event" is shown in Fig. 13(b). It is shown that IDSs are clearly present from "Start Event" fluctuation. Expanded window for "Large Load Change Event" is shown in Fig. 13(c).

It is shown that PhF reveals the existence of IDS's during the system load variation. An expanded window for PhF during "Intentional Islanding Event" is shown in Fig. 13(d). Results show that using PhF limits the detrimental impact of
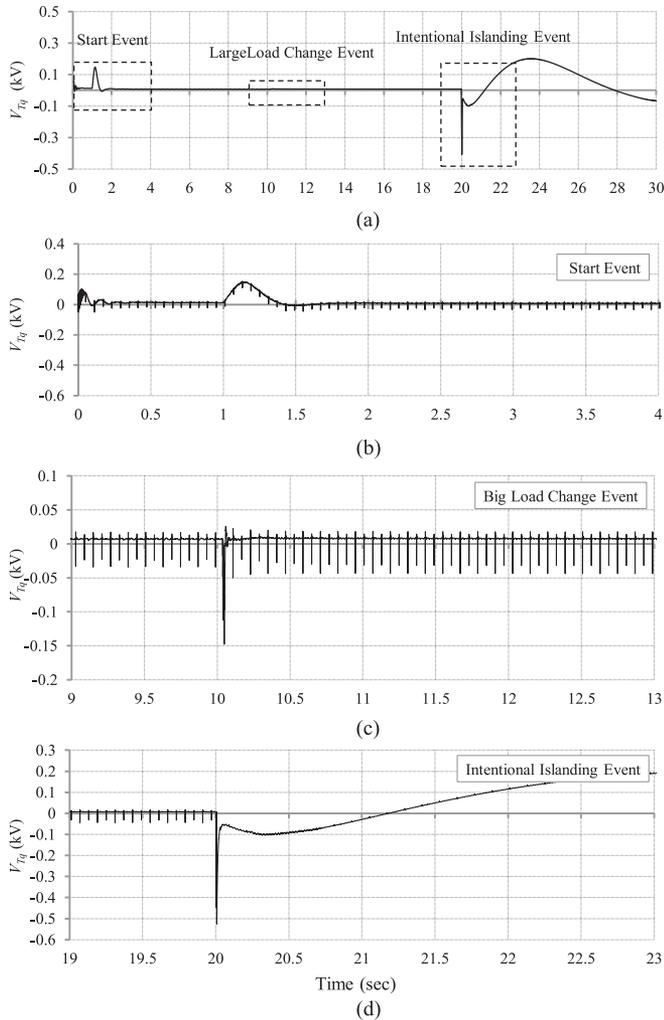
Fig. 12. (a) Full window of PCC voltage in *d–q* frame, (b) start event, (c) large load variation, and (d) islanding phenomenon.

the voltage fluctuation on IDS's extraction and makes them visible during the events. Using (2), the strength of the signal is calculated as $k = 0.83$. Comparison of the calculated k for the proposed method with the $k = 4\%$ in [39] and [40] reveals the significant improvement on signal extraction by the proposed method. Moreover, to ensure that the injected IDSs do not have negative impact on the system, THD level at the SG connection point is presented in Fig. 14. Results show that the maximum THD is less than 5% and conforms the IEEE Std. 1547.

B. Control of Island

Master–slave concept is applied to the generators with DG-1 as slave and DG-2 as master. Thus, when islanding occurs, DG-1 supplies P and Q to the load based on its droop settings. Meanwhile, DG-2 is responsible for maintaining the bus voltage, operating in *P-V* control mode. Hence, the master generator should be able to work ±10% of its rated value for 20–30 min [39]. Each generator shall be able to operate up to 0.8 lagging PF. Besides, active power output for DG-1 is 1.7 MW while DG-2 operates at 1.87 MW. Maximum reactive power output for DG-
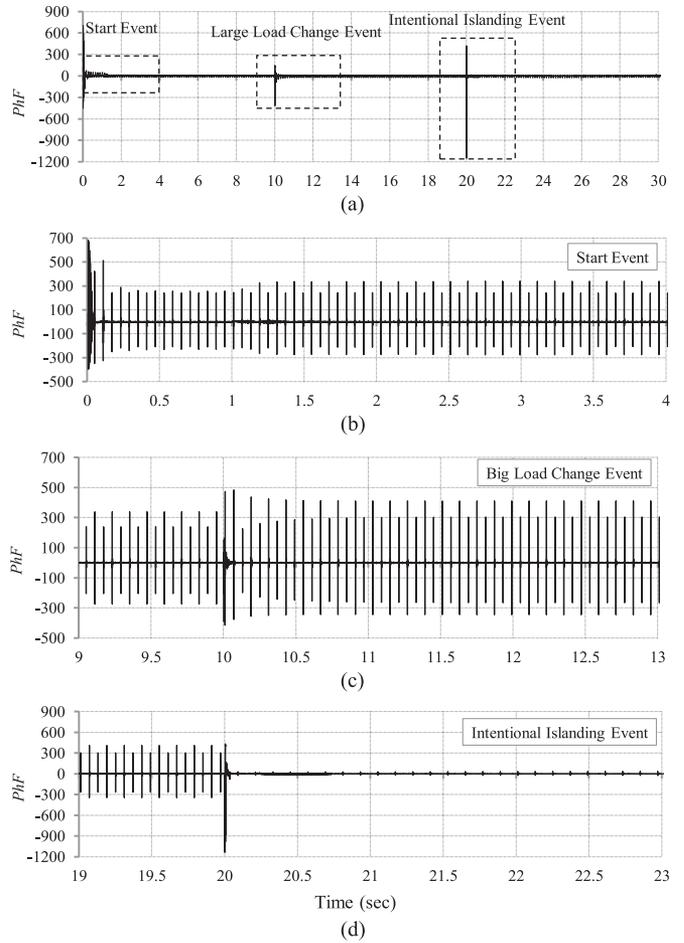
Fig. 13. (a) Extracted IDS using the proposed phase factor, (b) expanded window for start event, (c) expanded window for big load variation, and (d) expanded window for islanding phenomenon.
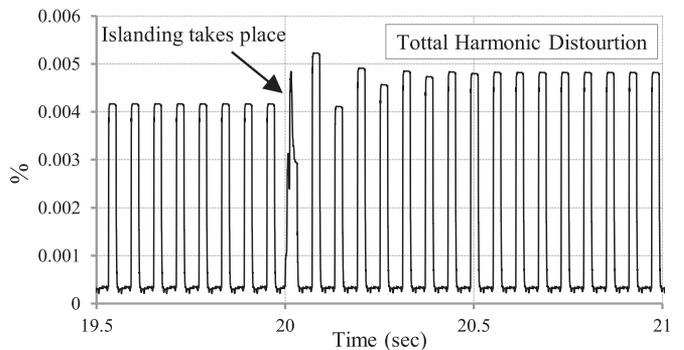
Fig. 14. THD at the main substation in the presence of the series of IDS.

1 is 1.053 MVAr and for DG-2 is 1.2 MVAr. DG-1 and DG-2 are capable of absorbing reactive power during under excitation mode. Maximum leading PF for DG-1 and DG-2 is 0.9. Droop setting for the governor of the DG units is calculated using (6). The droop coefficient is equal to $R_P = 1.87$. Moreover, droop coefficient for output reactive power is equal to $R_Q = 0.608$. The purpose of this case study is to verify the performance of the combination of the hybrid IDM and adaptive PI control system
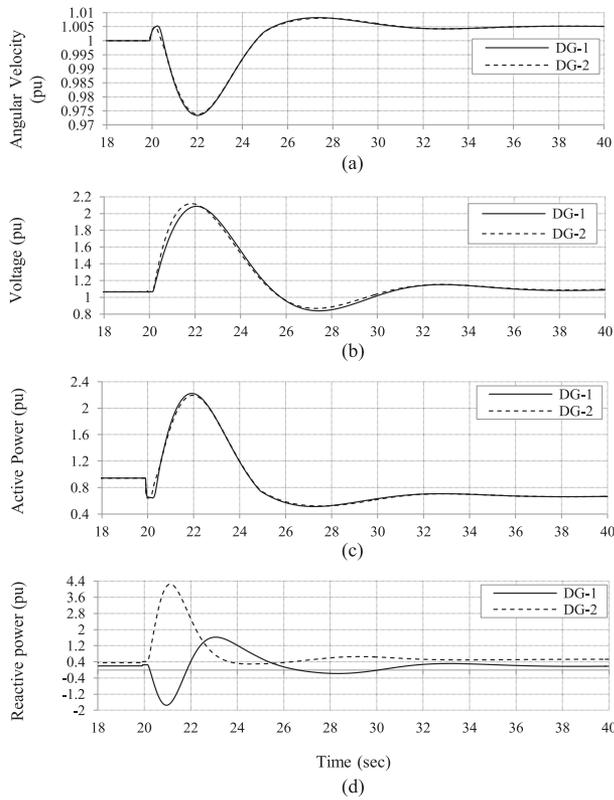
Fig. 15.   (a)–(d) Output characteristics of DG-1 and DG-2 using fix PI controller. (a) Angular velocity of the generators. (b) Voltage at bus 13. (c) Output active power. (d) Output reactive power.
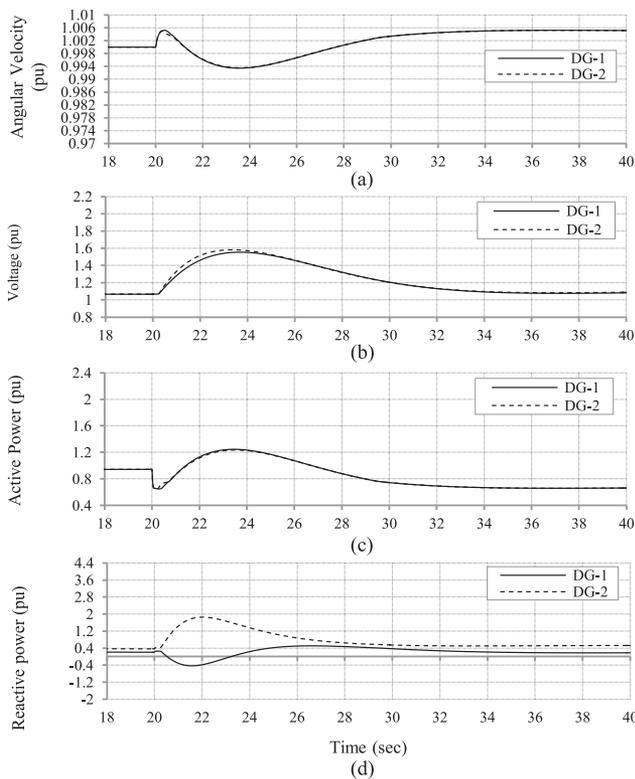

Fig. 16.   (a)–(d) Speed, voltage, active and reactive power of DG-1 and DG-2 using the adaptive PI controller.
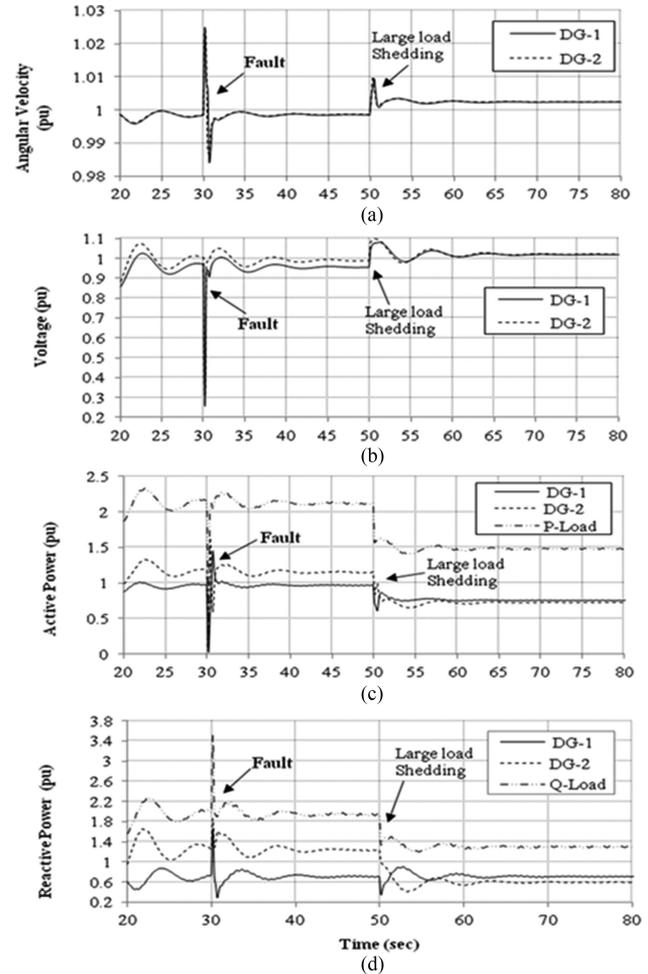
Fig. 17.   (a) Angular velocity, (b) voltage at PCC, (c) output active power, and (d) output reactive power for both DG units when contingencies occur during the autonomous operation using fix PI controller.

C. Control Strategy During Transition to Islanding

When islanding takes place due to the opening of the line L6 after 20 s, control system for DG-2 changes from *P-Q* to *P-V* mode while DG-1 remains in the *P-Q* mode. IWS from the SD is used to change the control mode of DG-2. After islanding, the load in the active island (feeder 2) is equal to $P = 2.67$ MW and $Q = 1.3$ MVAr. Fixed PI controller setting for both DG-1 and DG-2 are $K_p = 2$ and $T_i = 0.4$. The generator output parameters using fixed PI controller are shown in Fig. 15(a)–(d). Fig. 15(a) shows the under shoot for the angular velocity of two generators. The voltage fluctuation at PCC (Bus 13) is shown in Fig. 15(b). Active and reactive power fluctuations are demonstrated in Fig. 15(c) and (d). Results show that using the fixed PI controllers result in substantial oscillation on DG output parameters before they settle to their final value. In order to eliminate the oscillation and find the optimized value for K_p and T_i, each adaptive PI controller is controlled by two auxiliary PI controllers. By accomplishing adaptive controller, the adaptive PI controller could work more flexibly and can be retuned automatically for the new situation.
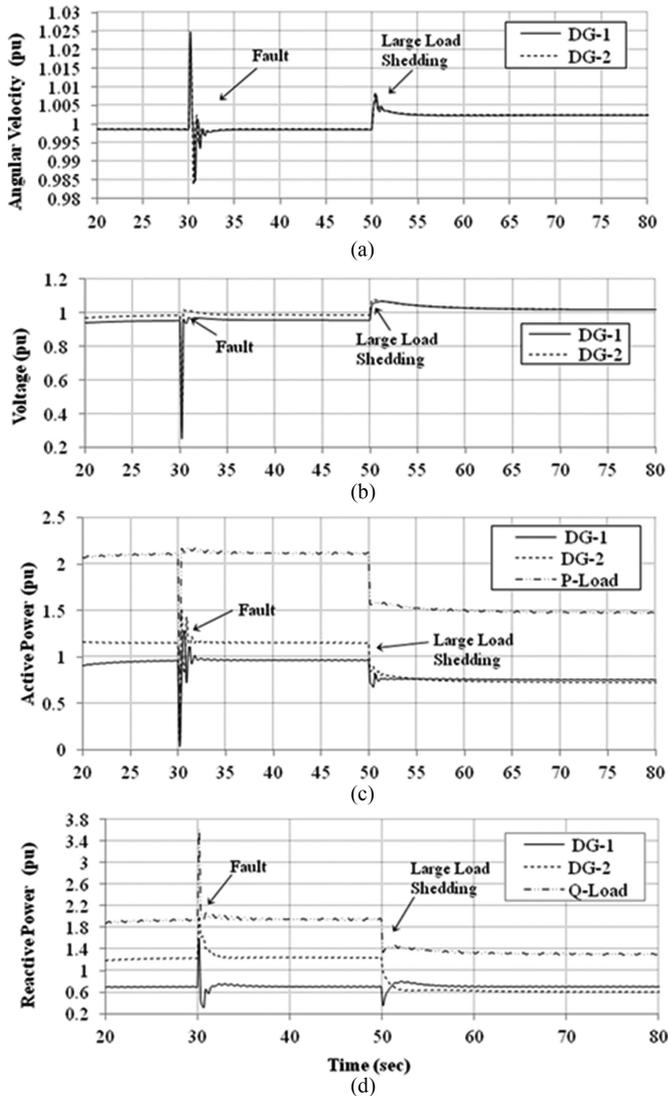
Fig. 18. (a) Angular velocity, (b) voltage at PCC, (c) output active power, and (d) output reactive power for both DG units when contingencies occur during the autonomous operation using the adaptive PI controller.

Fig. 16(a)–(d) indicates the output parameters for DG-1 and DG-2 utilizing adaptive controllers. Comparison of Figs. 15(a)–(d) and 16(a)–(d) shows significant improvement in both DG units' output parameters. Comparison between Figs. 15(a) and 16(a) reveals that the proposed adaptive PI controller decreases the undershoot of angular velocity. As seen in Fig. 15(b), the maximum overshoot of the voltage during the transition period is more than 2.1 p.u. when conventional fix PI controller is used. However, as shown in Fig. 16(b), the overshoot of the voltage is reduced to less than 1.6 p.u using the proposed control method. Moreover, adaptive PI controller decreases the active and reactive power oscillations considerably as compared to the conventional method as seen in Figs. 15(c) and (d) and 16(c) and (d).

D. Control Strategy During Autonomous Operation

In order to investigate the capability of the proposed control strategy to stabilizing the system during the autonomous
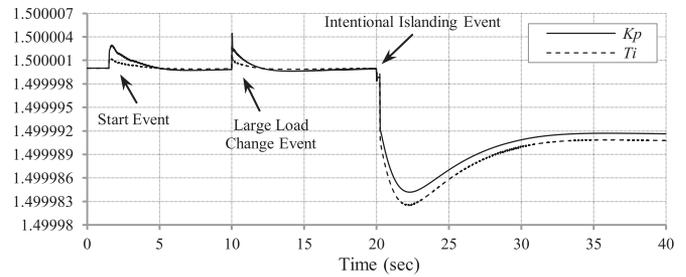

Fig. 19. Optimized value of K_p and T_i using rate of change of error.

operation, a three phases fault to ground and a large load shedding is applied to the system. Three phases to ground fault is added to the Bus13 since the generators are connected in this busbar. Moreover, in order to investigate the impact of large load changes on the proposed control strategy, Bus 7, 8, 9, and 10 have been shedded at 50 s. In Fig. 17(a)–(d), the network parameters such as angular velocity of the generators, busbar voltages, active and reactive power are shown when the conventional PI controller is used. As seen in Fig. 17, contingencies like fault and large load variation cause fluctuation in the hybrid system, which can lead to the unstable operating. In order to decrease the fluctuation and get the more stable operation, the proposed adaptive PI controller is used to control the DG units.

The network parameters with the adaptive PI controller are shown in Fig. 18(a)–(d). As shown in Fig. 18, generator output settles down to the pre-set values with very small fluctuation and settling time. In order to investigate the effectiveness of using error rates and adaptive PI controller to stabilize the system, adaptive PI controller parameters for *P-Q* control loop are presented in Fig. 18. According to Fig. 9(a), adaptive PI controller parameters, K_p and *Ti* are adjusted dynamically to decrease the active and reactive power error rates. Variation of the adaptive PI controller parameters to keep the output power of the DG-1 constant during different contingencies such as "Start Event," "Large Load Change Event," and "Intentional Islanding Event" are shown in Fig. 19.

VI. CONCLUSION

This paper proposed a new hybrid IDM along with an adaptive control strategy to enhance the system operation during the autonomous mode. The proposed IDM utilizes the ROCOVP to extract the IDSs sent from the main substation. The proposed detection method is capable of extracting the weaker IDSs compared to the existing methods. The ability to detect low strength signals results in smaller signal distortion by the SG. Hence, the power quality will improve with the proposed method. Moreover, the ability to detect low strength signals facilitate the use of lower rated equipments in the SG, which decreases the cost. Furthermore, the proposed IDM can be implemented in distribution systems to include both inverter-based and synchronous generator-based DG units. Second, to stabilize the system and smooth transition from grid-connected mode to islanding mode, an adaptive control strategy using various rates of errors is proposed in this paper. The proposed control architecture decreases

the overshoot, undershoot, and settling times of the DG parameters which result in the DG units remain stable during transition period. Moreover, the proposed adaptive control strategy confirms the DG unit's stable operation when various contingencies such as faults and large load variations occur in the system during autonomous operation mode.

REFERENCES

[1] *IEEE Standard for Interconnecting Distributed Resources with Electric Power Systems*, IEEE Standard 1547-2003, Jul. 28, 2003.

[2] B. Yu, M. Matsui, and G. Yu, "A review of current anti-islanding methods for photovoltaic power system," *Sol. Energy*, vol. 84, pp. 745–754, May 2010.

[3] Y. Zhihong, A. Kolwalkar, Y. Zhang, D. Pengwei, and R. Walling, "Evaluation of anti-islanding schemes based on nondetection zone concept," in *Proc. 2003 IEEE 34th Annu. Power Electron. Spec. Conf.*, 2003, vol. 4, pp. 1735–1741.

[4] F. Wang and Z. Mi, "Notice of retraction passive islanding detection method for grid connected PV system," in *Proc. Int. Conf. Ind. Inf. Syst. 2009*, 2009, pp. 409–412.

[5] H. Zeineldin and J. L. Kirtley Jr., "A simple technique for islanding detection with negligible nondetection zone," *IEEE Trans. Power Del.*, vol. 24, no. 2, pp. 779–786, Apr. 2009.

[6] A. Khamis, H. Shareef, E. Bizkevelci, and T. Khatib, "A review of islanding detection techniques for renewable distributed generation systems," *Renewable Sustain. Energy Rev.*, vol. 28, pp. 483–493, 2013.

[7] S. Syamsuddin, N. Rahim, and J. Selvaraj, "Implementation of TMS320-F2812 in islanding detection for photovoltaic grid connected inverter," in *Proc. 2009 Int. Conf. Tech. Postgraduates*, 2009, pp. 1–5.

[8] N. Lidula and A. Rajapakse, "A pattern recognition approach for detecting power islands using transient signals—Part I: Design and implementation," *IEEE Trans. Power Del.*, vol. 25, no. 4, pp. 3070–3077, Oct. 2010.

[9] J. Laghari, H. Mokhlis, M. Karimi, A. Bakar, and H. Mohamad, "Computational intelligence based techniques for islanding detection of distributed generation in distribution network: A review," *Energy Convers. Manage.*, vol. 88, pp. 139–152, 2014.

[10] H. Zeineldin, E. F. El-Saadany, and M. Salama, "Impact of DG interface control on islanding detection and nondetection zones," *IEEE Trans. Power Del.*, vol. 21, no. 3, pp. 1515–1523, Jul. 2006.

[11] C. Li, C. Cao, Y. Cao, Y. Kuang, L. Zeng, and B. Fang, "A review of islanding detection methods for microgrid," *Renewable Sustain. Energy Rev.*, vol. 35, pp. 211–220, 2014.

[12] S. Raza, H. Mokhlis, H. Arof, J. Laghari, and L. Wang, "Application of signal processing techniques for islanding detection of distributed generation in distribution network: A review," *Energy Convers. Manage.*, vol. 96, pp. 613–624, 2015.

[13] D. Velasco, C. L. Trujillo, G. Garcerá, and E. Figueres, "Review of anti-islanding techniques in distributed generators," *Renewable Sustain. Energy Rev.*, vol. 14, pp. 1608–1614, Aug. 2010.

[14] N. Lidula and A. D. Rajapakse, "A pattern-recognition approach for detecting power islands using transient signals—Part II: Performance evaluation," *IEEE Trans. Power Del.*, vol. 27, no. 3, pp. 1071–1080, Jul. 2012.

[15] W. Freitas, W. Xu, C. M. Affonso, and Z. Huang, "Comparative analysis between ROCOF and vector surge relays for distributed generation applications," *IEEE Trans. Power Del.*, vol. 20, no. 2, pp. 1315–1324, Apr. 2005.

[16] O. Raipala, A. Makinen, S. Repo, and P. Jarventausta, "The effect of different control modes and mixed types of DG on the non-detection zones of islanding detection," in *Proc. 2012 Workshop Integr. Renewables Distrib. Grid*, 2012, pp. 1–4.

[17] K. N. E. Ku Ahmad, J. Selvaraj, and N. A. Rahim, "A review of the islanding detection methods in grid-connected PV inverters," *Renewable Sustain. Energy Rev.*, vol. 21, pp. 756–766, May 2013.

[18] M. Ropp, J. Ginn, J. Stevens, W. Bower, and S. Gonzalez, "Simulation and experimental study of the impedance detection anti-islanding method in the single-inverter case," in *Proc. Conf. Rec. 2006 IEEE 4th World Conf. Photovolt. Energy Convers.*, 2006, pp. 2379–2382.

[19] P. O'Kane and B. Fox, "Loss of mains detection for embedded generation by system impedance monitoring," in *Proc. 6th Int. Conf. Develop. Power Syst. Protection*, 1997, pp. 95–98.

[20] H. Mohamad, H. Mokhlis, and H. W. Ping, "A review on islanding operation and control for distribution network connected with small hydro power plant," *Renewable Sustain. Energy Rev.*, vol. 15, pp. 3952–3962, 2011.

[21] A. Balaguer, X. I. J. lvarez, and E. I. Ortiz-Rivera, "Survey of distributed generation islanding detection methods," *IEEE Latin Amer. Trans.*, vol. 8, no. 5, pp. 565–570, Sep. 2010.

[22] M. Hanif, M. Basu, and K. Gaughan, "A discussion of anti-islanding protection schemes incorporated in a inverter based DG," in *Proc. 2011 10th Int. Conf. Environ. Elect. Eng.*, 2011, pp. 1–5.

[23] M. Ropp, M. Begovic, and A. Rohatgi, "Analysis and performance assessment of the active frequency drift method of islanding prevention," *IEEE Trans. Energy Convers.*, vol. 14, no. 3, pp. 810–816, Sep. 1999.

[24] L. A. Lopes and H. Sun, "Performance assessment of active frequency drifting islanding detection methods," *IEEE Trans. Energy Convers.*, vol. 21, no. 1, pp. 171–180, Mar. 2006.

[25] W. Y. Teoh and C. W. Tan, "An overview of islanding detection methods in photovoltaic systems," *World Acad. Sci. Eng. Technol.*, vol. 58, pp. 674–682, 2011.

[26] G. A. Smith, P. A. Onions, and D. G. Infield, "Predicting islanding operation of grid connected PV inverters," *Proc. Inst. Elect. Eng.–Elect. Power Appl.*, vol. 147, pp. 1–6, 2000.

[27] H. H. Zeineldin and M. M. A. Salama, "Impact of load frequency dependence on the NDZ and performance of the SFS islanding detection method," *IEEE Trans. Ind. Electron.*, vol. 58, no. 1, pp. 139–146, Jan. 2011.

[28] F. Liu, Y. Kang, Y. Zhang, S. Duan, and X. Lin, "Improved SMS islanding detection method for grid-connected converters," *IET Renewable Power Gener.*, vol. 4, pp. 36–42, 2010.

[29] K. N. E. K. Ahmad, J. Selvaraj, and N. A. Rahim, "A review of the islanding detection methods in grid-connected PV inverters," *Renewable Sustain. Energy Rev.*, vol. 21, pp. 756–766, 2013.

[30] D. Velasco, C. Trujillo, G. Garcera, and E. Figueres, "An active anti-islanding method based on phase-PLL perturbation," *IEEE Trans. Power Electron.*, vol. 26, no. 4, pp. 1056–1066, Apr. 2011.

[31] G.-K. Hung, C.-C. Chang, and C.-L. Chen, "Automatic phase-shift method for islanding detection of grid-connected photovoltaic inverters," *IEEE Trans. Energy Convers.*, vol. 18, no. 1, pp. 169–173, Mar. 2003.

[32] International Energy Agency, "Evaluation of islanding detection methods for photovoltaic utility interactive power systems," Int. Energy Agency, Paris France, Tech. Rep. IEA PVPS T5-09, 2002.

[33] J.-H. Kim, J.-G. Kim, Y.-H. Ji, Y.-C. Jung, and C.-Y. Won, "An islanding detection method for a grid-connected system based on the Goertzel algorithm," *IEEE Trans. Power Electron.*, vol. 26, no. 4, pp. 1049–1055, Apr. 2011.

[34] J. W. Stevens III, R. H. Bonn, J. W. Ginn, S. Gonzalez, and G. Kern, *Development and Testing of an Approach to Anti-islanding in Utility-Interconnected Photovoltaic Systems*. Albuquerque, NM, USA: Sandia Nat. Lab., 2000.

[35] J. Yin, L. Chang, and C. Diduch, "Recent developments in islanding detection for distributed power generation," in *Proc. 2004 Large Eng. Syst. Conf. Power Eng.*, 2004, pp. 124–128.

[36] V. Menon and M. H. Nehrir, "A review of issues regarding the use of distributed generators," in *Proc. 37th Annu. North Amer. Power Symp. 2005*, 2005, pp. 399–405.

[37] M. A. Redfern, O. Usta, and G. Fielding, "Protection against loss of utility grid supply for a dispersed storage and generation unit," *IEEE Trans. Power Del.*, vol. 8, no. 3, pp. 948–954, Jul. 1993.

[38] W. Gao, "Comparison and review of islanding detection techniques for distributed energy resources," in *Proc. 2008 40th North Amer. Power Symp.*, 2008, pp. 1–8.

[39] W. Xu, G. Zhang, C. Li, W. Wang, G. Wang, and J. Kliber, "A power line signaling based technique for anti-islanding protection of distributed generators—Part I: Scheme and analysis," *IEEE Trans. Power Del.*, vol. 22, no. 3, pp. 1758–1766, Jul. 2007.

[40] W. Wang, J. Kliber, G. Zhang, W. Xu, B. Howell, and T. Palladino, "A power line signaling based scheme for anti-islanding protection of distributed generators—Part II: Field test results," *IEEE Trans. Power Del.*, vol. 22, no. 3, pp. 1767–1772, Jul. 2007.

[41] F. De Mango, M. Liserre, and A. Dell'Aquila, "Overview of anti-islanding algorithms for PV systems. Part II: ActiveMethods," in *Proc. 2006 12th Int. Power Electron. Motion Control Conf. 2006*, 2006, pp. 1884–1889.

[42] D. Velasco, C. Trujillo, G. Garcerá, and E. Figueres, "Review of anti-islanding techniques in distributed generators," *Renewable Sustain. Energy Rev.*, vol. 14, pp. 1608–1614, 2010.

[43] M. Khodaparastan, H. Vahedi, F. Khazaeli, and H. Oraee, "A novel hybrid islanding detection method for inverter-based DGs using SFS and ROCOF," *IEEE Trans. Power Del.*, vol. 32, no. 5, pp. 2162–2170, Oct. 2017.

[44] S. D. Kermany, M. Joorabian, S. Deilami, and M. A. S. Masoum, "Hybrid islanding detection in microgrid with multiple connection points to smart grids using fuzzy-neural network," *IEEE Trans. Power Syst.*, vol. 32, no. 4, pp. 2640–2651, Jul. 2017.

[45] M. Karimi, H. Mokhtari, and M. R. Iravani, "Wavelet based on-line disturbance detection for power quality applications," *IEEE Trans. Power Del.*, vol. 15, no. 4, pp. 1212–1220, Oct. 2000.

[46] Y. Gu and M. H. Bollen, "Time-frequency and time-scale domain analysis of voltage disturbances," *IEEE Trans. Power Del.*, vol. 15, no. 4, pp. 1279–1284, Oct. 2000.

[47] F. Katiraei, M. R. Iravani, and P. W. Lehn, "Micro-grid autonomous operation during and subsequent to islanding process," *IEEE Trans. Power Del.*, vol. 20, no. 1, pp. 248–257, Jan. 2005.

[48] C. N. Rowe, T. J. Summers, R. E. Betz, D. J. Cornforth, and T. G. Moore, "Arctan power–frequency droop for improved microgrid stability," *IEEE Trans. Power Electron.*, vol. 28, no. 8, pp. 3747–3759, Aug. 2013.

[49] P. G. Arul, V. K. Ramachandaramurthy, and R. K. Rajkumar, "Control strategies for a hybrid renewable energy system: A review," *Renewable Sustain. Energy Rev.*, vol. 42, pp. 597–608, Feb. 2015.

[50] T. N. Berhad, *Malaysian Distribution Code*, 2010.

[51] W. Wencong, J. Kliber, Z. Guibin, X. Wilsun, B. Howell, and T. Palladino, "A power line signaling based scheme for anti-islanding protection of distributed generators: Part II: Field test results," in *Proc. IEEE Power Eng. Soc. Gen. Meeting 2007*, 2007, p. 1.

[52] B. C. Kuo, *Automatic Control Systems*. Upper Saddle River, NJ, USA: Prentice-Hall, 1981.

Vigna K. Ramachandaramurthy (SM'12) received the Ph.D. degree from the University of Manchester Institute of Science and Technology, Manchester, U.K., in 2001.

He is currently a Professor and heads the Power Quality Research Group, Tenaga National University, Kajang, Malaysia. His main research interests include power system studies, power system protection, power quality, renewable energy integration, and grid impact of distributed generation.

Nadarajah Mithulananthan (SM'10) received the Ph.D. degree in electrical and computer engineering from the University of Waterloo, Waterloo, ON, Canada, in 2002.

He was an Electrical Engineer with the Generation Planning Branch, Ceylon Electricity Board, Sri Lanka, and a Researcher with Chulalongkorn University, Bangkok, Thailand. He also served as an Associate Professor with the Asian Institute of Technology, Bangkok. He is currently with the School of Information Technology and Electrical Engineering, University of Queensland, Brisbane, QLD, Australia. His main research interests include renewable energy integration and grid impact of distributed generation, electric-vehicle charging, and energy-storage systems.

Aref Pouryekta (S'13) received the Ph.D. degree in electrical engineering from Tenaga National University, Kajang, Malaysia, in 2017.

He is currently a Postdoctoral Research Fellow with Tenaga National University. His research interests include renewable energy integration, microgrid stability, and power system modeling.

Atputharajah Arulampalam (SM'09) received the B.Sc.Eng. degree (with first class honors) from the University of Peradeniya, Peradeniya, Sri Lanka, in 1997, and the Ph.D. degree from the University of Manchester Institute of Science and Technology, Manchester, U.K., in 2003.

He is currently a Professor and, since June 2015, has served as the Dean of the Faculty of Engineering, University of Jaffna, Jaffna, Sri Lanka. His main research interests include renewable energy, microgrids and power electronic control systems.